High-Pressure Synthesis of Boron-Doped Ultrasmall Diamonds from an Organic Compound

*Evgeny A. Ekimov, Oleg S. Kudryavtsev, Andrey A. Khomich, Oleg I. Lebedev, Tatiana A. Dolenko, and Igor I. Vlasov**

A new wave of interest in diamond as a high-tech material comes from the discovery of the remarkable spin, luminescent, and conductive properties of doped diamond. Long-living spin states of point defect related to nitrogen impurity in diamond have been revealed.[1] This property offers the prospect of constructing quantum information bits based on nitrogen-related defects in diamond and its application as an information carrier in spintronics, quantum computing, and quantum cryptography.[2] The high emission rate, stability, and high quantum yield of luminescence inherent in a number of impurity defects (color centers) in diamond allowed us to reliably detect emissions from a laser-stimulated single defect in a diamond at room temperature.[3] This property makes the diamond a promising material for the construction of highly efficient and relatively simple single-photon sources. Recently superconductivity, a property unexpected for wide bandgap semiconductors, was found in diamond heavily doped with boron.[4,5] The new spin, fluorescent, and conductive properties were discovered first in bulk diamond doped with certain impurity atoms. Currently, these properties are actively introduced into nanocrystalline diamonds to significantly empower their use. Nanomagnetometers, conducting biosensors, and single-photon emitters are already implemented thanks to diamond nanoparticles doped with nitrogen, boron, and silicon.[3,6,7] However, the transition to the nanoscale level is challenging because of the lack of high structural quality of nanodiamonds (NDs) and methods for their controllable doping.

Common methods for the direct synthesis of nanodiamonds, such as detonation[8,9] laser ablation,[10] and others, are based on dynamic synthesis which happens in a short time (milliseconds and less) under strongly nonequilibrium and poorly controlled temperature and pressure, which determine the structural form and solubility of impurity defects in diamond.[11,12] There is limited information in literature on application of the high pressure–high temperature (HPHT) technique, in which diamond synthesis is realized under controllable pressure and temperature, for the direct synthesis of nanodiamond from hydrocarbons. Note that the pioneer of diamond synthesis from hydrocarbons at high pressures is R. H. Wentorf who reported in his seminal paper[13] the production of unusually "soft" ("not scratching the glass") diamond. Broad X-ray diffraction lines indicated the formation of nanocrystalline diamond. Later, Onodera et al.[14] have shown that nanodiamond can be obtained at lower pressures and temperatures than those used by Wentorf. Undoped nanodiamonds were obtained at a pressure of 8 GPa and temperatures of 1100–1600 K from camphene ($C_{10}H_{16}$). According to transmission electron microscopy (TEM) analysis the elementary crystallite size was less than 10 nm, but they were coagulated. The coagulation yielded flat platelets larger than 100 μm across. We also note the recent work on synthesis of diamond nanocrystals with a size of a few nanometers in the C–N system (under C_3N_4 decomposition).[15] The presence of nitrogen impurity in those ND was not reported. At the same time, the very high pressure (15–25 GPa) of the synthesis and the small size of the platinum capsule used for the sample production exclude the practical significance of this method for the ND synthesis. Recently, the preparation of heterogeneous size diamond particles (including nanoscaled) doped with silicon during their synthesis from mixtures of hydrocarbon and fluorocarbon compounds was also reported.[16] In general, the use of mixtures of reactants for the synthesis of small diamonds cannot provide the required uniformity in diamond doping level and crystal size.

Until now, an indirect approach, such as top-down is used for the production of doped ND. It consists of mechanical grinding of doped bulk diamond obtained by such methods as static synthesis as chemical vapour deposition (CVD) and HPHT.[17–20] This approach is a multistage and extremely labor-intensive. It is accompanied by sample contamination from milling beads and by surface graphitization.[20] The resulting product is grinding diamond nanoparticles with a polydisperse size distribution and splinter shape. The yield of small nanoparticles is extremely low. For nitrogen-doped nanodiamond the smallest size of 10 nm was still provided,[17] for boron-doped – 30 nm.[20]

In the present work, we propose the direct synthesis of doped nanodiamond based on HPHT treatment of a one-component precursor containing the dopant atom(s). The synthesis was implemented to obtain heavily boron-doped nanodiamond

Dr. E. A. Ekimov
Physics, RAS
Kaluzhskoe Road 14, Troitsk 142190, Russia
O. S. Kudryavtsev, A. A. Khomich, Dr. I. I. Vlasov
General Physics Institute
RAS
Vavilov Str. 38, Moscow 119991, Russia
E-mail: vlasov@nsc.gpi.ru
Dr. O. I. Lebedev
Laboratoire CRISMAT
UMR 6508 CNRS-ENSICAEN
6 Boulevard Marechal Juin 14050, Caen, France
Dr. T. A. Dolenko
Physics Department
Moscow State University
Leninskie Gory 1, Moscow 119991, Russia
Dr. I. I. Vlasov
National Research Nuclear University MEPhI
Kashirskoe Road 31, Moscow 115409, Russia

DOI: 10.1002/adma.201502672

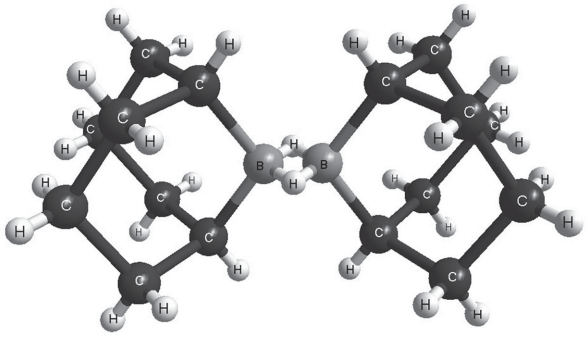

Figure 1. Structure of 9BBN molecule: The spatial arrangement of carbon atoms in 9BBN molecules resembles the structure of diamond.

(BDND) of smallest size. The production of ND particles doped with nitrogen, silicon, and other atoms by direct HPHT synthesis is in progress.

The HPHT synthesis was carried out from the organoboron compound 9-borabicyclo[3,3,1] nonane dimer (9BBN), $C_{16}H_{30}B_2$ (**Figure 1**), at a pressure of 8–9 GPa in a temperature range of 1200–2000 K (see the Experimental Section and Figure S1, Supporting Information, for details). The temperature of 1550 K was found to be the lowest at which three peaks of diamond phase, attributed to reflections from diamond lattice planes with indexes of (111), (220), and (311), are reliably detected in the X-ray diffraction pattern of the synthesized products (**Figure 2**). The diamond crystallite size calculated by Selyakov–Scherrer's formula is about 6 nm. Increase of the synthesis temperature results in an increase of the size of diamond crystallites (inset of Figure 2). At the synthesis temperature of 1950 K typical crystallite sizes reach 200–300 nm (Figure S2, Supporting Information). Along with diamond a graphite phase, decreasing in amount with temperature, is also detected in the samples. In addition, boron carbide becomes detectable in the sample synthesized at 1950 K (Figure 2).

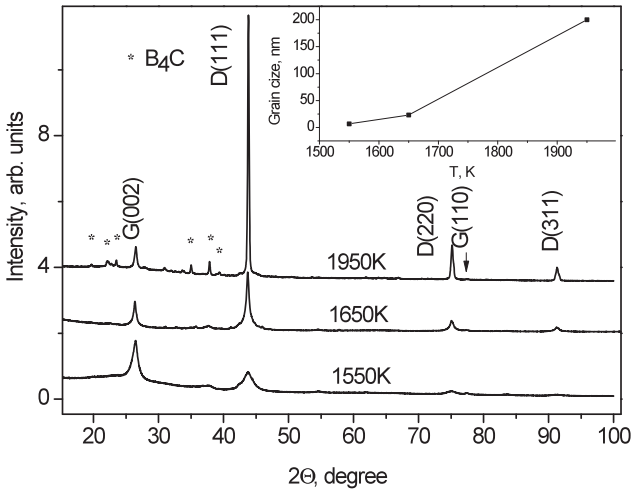

Figure 2. XRD analysis of NDs: Diffraction patterns of the samples synthesized at 1550 K, 1650 K, and 1950 K. D: diamond, G: graphite, and *: boron carbide (B_4C). Inset: Dependence of the diamond crystallite size on HPHT synthesis temperature.

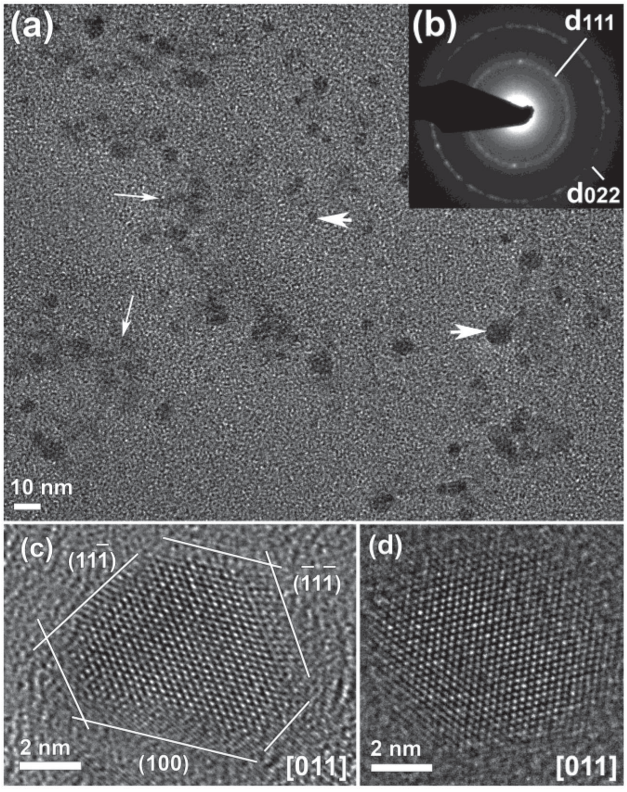

Figure 3. a) Bright field low-magnification TEM image of as-grown "1550 K" sample, diamond particles are marked with thick arrows and graphite nanostructures with thin arrows; b) ED ring pattern, two distinguished rings correspond to reflections from (111) and (220) diamond planes; and c,d) bright field high-resolution TEM image of diamond nanoparticles viewed along [110] zone axis. The particles in (c) have a truncated octahedral shape with mainly {111} surface plane, and {100}-type truncation.

Further characterization of the produced material was mostly focused on the smallest NDs obtained at 1550 K.

To identify the structure and morphology of the as-produced "1550 K" ND particles, they were analyzed by TEM. Bright field low-magnification TEM image of as-grown "1550 K" showed diamond particles (dark contrast) and formless graphite nanostructures (gray contrast), all diamond particles were below 10 nm in size (**Figure 3**a). The corresponding ring electron diffraction (ED) pattern (Figure 3b) confirms diamond structure of the particles with most pronounced reflections from (111) and (220) diamond lattice planes. It is apparent from the large number of high-resolution TEM (HRTEM) images taken, that the particles are highly crystalline and, in contrast to the detonation NDs,[21] are free of multiple twinning. HRTEM images of individual diamond particles are shown in Figure 3c,d. The particle displayed in Figure 3c shows a shape close to truncated octahedral faceting by {111} and {100} planes, whereas the particle in Figure 3d is close to spherical.

To evaluate the size distribution of the "1550 K" ND particles they were purified with acids, dispersed in water, and then analyzed by the dynamic light scattering (DLS) method. Note that ND particles are easily dispersed in water after their purification, forming bluish colloidal solution (**Figure 4** inset). The DLS

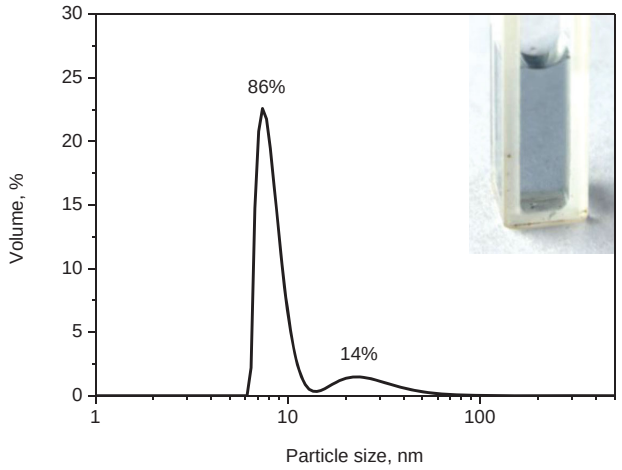

Figure 4. DLS analysis of smallest ND: Particle size distribution of "1550 K" sample suspension after purification. Inset: Bluish colloidal solution of purified "1550 K" sample.

analysis has shown monodisperse size distribution near 7 nm (Figure 4) for a majority of the particles (86% of the sample volume). We relate the small amount (14%) of larger (10–50 nm) diamond particles to still nonuniform synthesis conditions within the capsule volume or/and to small particle aggregates.

To determine the boron incorporation efficiency into the diamond lattice the Raman analysis was applied to the purified "1550 K" and untreated "1950 K" samples. The Raman spectra of the "1550 K" diamond powder dried from the water suspension and untreated "1950 K" diamond powder were characteristic for a heavily boron-doped diamond (**Figure 5**a). The diamond line belonging to the zone-center phonon mode is shifted from 1332 cm^{-1} (observed for undoped diamond) down to 1310 cm^{-1}. There is an empirical relation between the diamond line shift and the concentration of substitutional boron atoms in the diamond lattice[22] which allows us to estimate the boron concentration in "1550 K" diamond at the level of 1 at%. In the "1950 K" sample, a similar substitutional boron concentration of 1 at% was determined through the value of the lattice constant (see the Supporting Information). The lines of both spectra positioned below 1300 cm^{-1} are ascribed to vibration modes of C and B in diamond lattice.[23] The positions of these lines are different in two shown spectra, probably, due to the size confinement effect, manifested in the smallest diamond particles.[24] This is a subject for further investigation of the produced material. The weak line at 1600 cm^{-1} indicates that sp^2-bonded carbon was not completely removed from the "1550 K" sample during its acid purification. Excellent reproducibility of the Raman spectra measured in different point of the "1550 K" diamond powder reveals homogeneous distribution of the boron within the diamond nanoparticles of the whole sample. The presence of boron atoms in the starting material at a molecular level facilitates the uniform doping of diamond with boron.

The photoluminescence (PL) spectrum of the "1550 K" sample shows an intense broad line centered around 550 nm (Figure 4b), which is a fingerprint of any ultrasmall nanodiamond powder. This PL band is observed in detonation, meteoritic, milled HPHT NDs and relates to structural defects of the diamond surface.[25–27] The line becomes especially pronounced

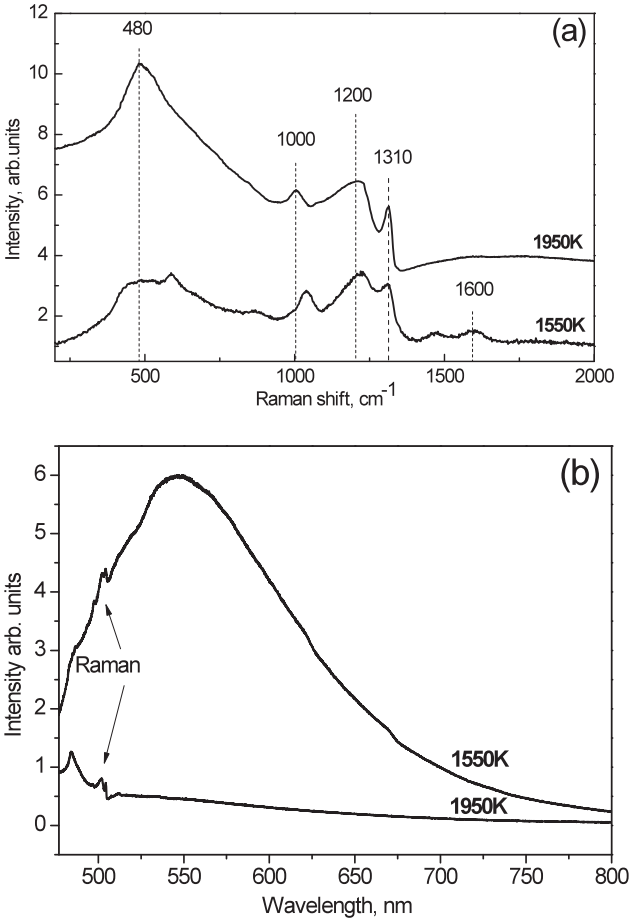

Figure 5. Raman and PL analysis of NDs: a) Raman and b) PL spectra of "1550 K" and "1950 K" samples. Raman spectrum of "1550 K" is shown after PL background subtraction.

in NDs with sizes of below 10 nm, for which the ratio of surface/volume carbon atoms is essential. In contrast to "1550 K" sample, no PL emission was observed from large particles of "1950 K" sample, which is typical for B-doped bulk diamond.

Based on the obtained results we conclude that a key point of the direct synthesis of doped nanodiamond is the use of one-component organic compound containing hydrocarbon in sp^3 configuration and dopant atoms. It is known that the pressure of about 11 GPa is borderline, when graphite and other carbon materials undergo the direct conversion to diamond. At lower pressures (we operated at 8–9 GPa) the diamond formation is possible if one reduces the potential barrier of the carbon transformation. This can be achieved by using a starting material close to the structure of the diamond. In this regard, the carbon skeleton of molecules 9BBN is essentially a ready building block of the diamond lattice (Figure 1). Probably, hydrogen is also an important element of the ND synthesis, which stabilizes carbon in sp^3 configuration. The presence of boron atoms in the carbon cycle directly facilitates the doping of diamond with boron. Increasing the size of diamond crystals with synthesis temperature is consistent with the concept of the nucleation and growth of crystals: at low temperatures the process of homogeneous nucleation of

diamond prevails, while crystal growth dominates at higher temperature.

Here, the ability to control the size of diamond crystals in the range 7–200 nm, varying the synthesis temperature was demonstrated. The next step in developing B-doped ND synthesis will be to learn how to control the concentration of boron in this material. This can be obtained by changing the synthesis conditions, such as pressure, and by changing the relative content of boron in the precursor.

In conclusion, we have found a direct route for the production of doped nanodiamond with variable size down to less than 10 nm. It consists in the HPHT treatment of an sp^3-configured organic compound containing dopant, and allows producing relatively large amount (100 mg per 5 min cycle) of doped nanodiamond which makes this material easily accessible for nanotechnological applications. In an exemplary implementation of the new route, diamond nanoparticles with a size below 10 nm, containing a high concentration of substitutional boron (≈1%), have been produced by HPHT treatment of 9BBN molecules. The material is well powdered and easily dispersed in water, forming the utmost stable water suspension. Heavily BDND is of great interest for fundamental science. As it is well known, heavily boron-doped diamond becomes superconducting at liquid helium temperatures with electrons forming Cooper pairs with calculated size (the coherence length) of about 10 nm. Studying the conducting properties of the heavily BDND of different sizes, offers a unique opportunity to retrieve the coherence length of a Cooper pair in diamond experimentally. Prospective nanotechnological applications of BDND powder are foreseen in the use of this material as a support for various catalysts[28] as a conductive ink in screen-printed technologies,[29] among others. Our finding opens a new era of direct production of nanodiamond with particle size and impurity content on demand.

Experimental Section

To create high pressures and temperatures, an apparatus of uniaxial compression and the high-pressure chamber of "toroid-15" type were used. The 9BBN compound (white crystals with melting point 426–428 K, 98% Aldrich Chem. Co.) in the form of pressed cylindrical pellets of 5 mm diameter and a height of 4 mm was encapsulated in Ti. The capsules were placed into a container made of ZrO_2 and $CaCO_3$. Pressing into the cylindrical pellet, placing the pellet into the synthesis cell and transportation of the synthesis cell to the high-pressure facility were performed in the atmosphere of dried argon of high purity (99.998%). The temperature (up to 1630 K) in the experiment was monitored using a chromel–alumel thermocouple junction which was placed on the wall of the capsule, in the middle of its height. The synthesis was performed at 8–9 GPa in temperatures range of 900–2000 K. The exposure time at constant parameters of synthesis was 60 s.

X-ray diffraction patterns were recorded with a powder diffractometer STADI MP (Stoe) using monochromatic Cu Kα1 radiation.

As-produced ND powder was purified with a mixture of concentrated nitric/sulfuric (1:3) acids for 2 h. Then the acids were substituted with doubly distilled water by 11 washing/centrifugation (LMC-3000, BioSan) cycles (15–30 min, 1700 g). The particle sizes of the ND water suspension were measured by dynamic light scattering (DLS; ALV-CGS 5000/6010).

HRTEM and ED analysis were performed on nanodiamond powder dispersed on a carbon grid using a JEM ARM200F probe and image aberration corrected microscope operated at 200 kV and equipped with CENTURIO EDX detector.

Raman and photoluminescence spectra of the nanodiamond powder were recorded at room temperature using a LABRAM HR800 spectrometer equipped with the diode-pumped solid-state laser Ciel-473 (Laser Quantum) for Raman and luminescence excitation. The laser beam (power, 0.1 mW; wavelength, 473 nm) was focused in a 2 μm spot on the surface of the ND powder dried from the water solution on an Si substrate. The spectrometer was operated in a confocal mode; a backscattering geometry was used for the Raman and PL spectra recording.

Supporting Information

Supporting Information is available from the Wiley Online Library or from the author.

Acknowledgements

This work was supported by the Russian Scientific Foundation (Grant No. 14-12-01329).

Received: June 4, 2015
Revised: July 13, 2015
Published online: August 18, 2015

[1] B. Naydenov, F. Dolde, L. T. Hall, C. Shin, H. Fedder, L. C. L. Hollenberg, F. Jelezko, J. Wrachtrup, *Phys. Rev. B* **2011**, *83*, 081201.
[2] M. D. Lukin, P. R. Hemmer, *Phys. Rev. Lett.* **2000**, *84*, 2818.
[3] I. Aharonovich, S. Castelletto, D. A. Simpson, C.-H. Su, A. D. Greentree, S. Prawer, *Rep. Prog. Phys.* **2011**, *74*, 076501.
[4] E. A. Ekimov, V. A. Sidorov, E. D. Bauer, N. N. Mel'nik, N. J. Curro, J. D. Thompson, S. M. Stishov, *Nature* **2004**, *428*, 542.
[5] G. Zhang, S. Turner, E. A. Ekimov, J. Vanacken, M. Timmermans, T. Samuely, V. A. Sidorov, S. M. Stishov, Y. Lu, B. Deloof, B. Goderis, G. Tendeloo, J. Vondel, V. V. Moshchalkov, *Adv. Mater.* **2014**, *26*, 2034.
[6] G. Balasubramanian, I. Y. Chan, R. Kolesov, M. Al-Hmoud, J. Tisler, C. Shin, C. Kim, A. Wojcik, P. R. Hemmer, A. Krueger, T. Hanke, A. Leitenstorfer, R. Bratschitsch, F. Jelezko, J. Wrachtrup, *Nature* **2008**, *455*, 648.
[7] S. Mandal, T. Bautze, O. A. Williams, C. Naud, E. Bustarret, F. Omnes, P. Rodiere, T. Meunier, C. Bauerle, L. Saminadayar, *ACS Nano* **2011**, *5*, 7144.
[8] N. R. Greiner, D. S. Phillips, J. D. Johnson, F. Volk, *Nature* **1988**, *333*, 440.
[9] V. Yu. Dolmatov, *Russ. Chem. Rev.* **2007**, *76*, 339.
[10] G. W. Yang, J. B. Wang, Q. X. Liu, *J. Phys. Condens. Matter* **1998**, *10*, 7923.
[11] A. T. Collins, H. Kanda, H. Kitawaki, *Diamond Relat. Mater.* **2000**, *9*, 113.
[12] H. Kanda, S. C. Lawson, *Ind. Diamond Rev.* **1995**, *55*, 56.
[13] R. H. Wentorf Jr., *J. Phys. Chem.* **1965**, *69*, 3063.
[14] A. Onodera, K. Suito, Y. Morigami, *Proc. Jpn. Acad., Ser. B* **1992**, *68*, 167.
[15] L. Fang, H. Ohfuji, T. Irifune, *J. Nanomater.* **2013**, *41*, 2013.
[16] V. A. Davydov, A. V. Rakhmanina, S. G. Lyapin, I. D. Ilichev, K. N. Boldyrev, A. A. Shiryaev, V. N. Agafonov, *JETP Lett.* **2014**, *99*, 585.

[17] J.-P. Boudou, J. Tisler, R. Reuter, A. Thorel, P. A. Curmi, F. Jelezko, J. Wrachtrup, *Diamond Relat. Mater.* **2013**, *37*, 80.
[18] E. Neu, C. Arend, E. Gross, F. Guldner, C. Hepp, D. Steinmetz, E. Zscherpel, S. Ghodbane, H. Sternschulte, D. Steinmüller-Nethl, Y. Liang, A. Krueger, C. Becher, *Appl. Phys. Lett.* **2011**, *98*, 243107.
[19] S. Heyer, W. Janssen, S. Turner, Y. G. Lu, W. S. Yeap, J. Verbeeck, K. Haenen, A. Krueger, *ACS Nano* **2014**, *8*, 5757.
[20] E. Neu, F. Guldner, C. Arend, Y. Liang, S. Ghodbane, H. Sternschulte, D. S. Nethl, A. Krueger, C. Becher, *J. Appl. Phys.* **2013**, *113*, 203507.
[21] S. Turner, O. I. Lebedev, O. Shenderova, I. I. Vlasov, J. Verbeeck, G. Van Tendeloo, *Adv. Funct. Mater.* **2009**, *19*, 2116.
[22] R. J. Zhang, S. T. Lee, Y. W. Lam, *Diamond Relat. Mater.* **1996**, *5*, 1288.
[23] E. Bourgeois, E. Bustarret, P. Achatz, F. Omnès, X. Blasé, *Phys. Rev. B* **2006**, *74*, 094509.
[24] J. W. AgerIII, D. K Veirs, G. M. Rosenblatt, *Phys. Rev. B* **1991**, *43*, 6491.
[25] L. Bergman, M. T. McClure, J. T. Glass, R. J. Nemanich, *J. Appl. Phys.* **1994**, *76*, 3020.
[26] R. Bradley, D. G. Smith, T. Plakhotnik, *Diamond Relat. Mater.* **2010**, *19*, 314.
[27] A. A. Shiryaev, A. V. Fisenko, I. I. Vlasov, L. F. Semjonova, P. Nagel, S. Schuppler, *Geochim. Cosmochim. Acta* **2011**, *75*, 3155.
[28] G. R. Salazar-Banda, K. I. B. Eguiluz, L. A. Avaca, *Electrochem. Commun.* **2007**, *9*, 59.
[29] T. Kondo, M. Horitani, H. Sakamoto, I. Shitanda, Y. Hoshi, M. Itagaki, M. Yuasa, *Chem. Lett.* **2013**, *42*, 352.